Bi-allelic HPDL Variants Cause a Neurodegenerative Disease Ranging from Neonatal Encephalopathy to Adolescent-Onset Spastic Paraplegia

Ralf Husain, Mona Grimmel, Matias Wagner, J. Christopher Hennings, Christian Marx, René Feichtinger, Abdelkrim Saadi, Kevin Rostásy, Florentine Radelfahr, Andrea Bevot, et al.

REPORT

Bi-allelic *HPDL* Variants Cause a Neurodegenerative Disease Ranging from Neonatal Encephalopathy to Adolescent-Onset Spastic Paraplegia

Ralf A. Husain,[1,31] Mona Grimmel,[2,31] Matias Wagner,[3,4,5] J. Christopher Hennings,[6] Christian Marx,[7] René G. Feichtinger,[8] Abdelkrim Saadi,[9] Kevin Rostásy,[10] Florentine Radelfahr,[11,12] Andrea Bevot,[13] Marion Döbler-Neumann,[13] Hans Hartmann,[14] Laurence Colleaux,[15] Isabell Cordts,[16] Xenia Kobeleva,[17] Hossein Darvish,[18] Somayeh Bakhtiari,[19] Michael C. Kruer,[19] Arnaud Besse,[20] Andy Cheuk-Him Ng,[21] Diana Chiang,[21] Francois Bolduc,[21] Abbas Tafakhori,[22] Shrikant Mane,[23] Saghar Ghasemi Firouzabadi,[24] Antje K. Huebner,[6] Rebecca Buchert,[2] Stefanie Beck-Woedl,[2] Amelie J. Müller,[2] Lucia Laugwitz,[2,13] Thomas Nägele,[25] Zhao-Qi Wang,[7,26] Tim M. Strom,[3,4] Marc Sturm,[2] Thomas Meitinger,[3,4,27] Thomas Klockgether,[17,28] Olaf Riess,[2,29] Thomas Klopstock,[11,12,27] Ulrich Brandl,[1] Christian A. Hübner,[6] Marcus Deschauer,[16] Johannes A. Mayr,[8] Penelope E. Bonnen,[20] Ingeborg Krägeloh-Mann,[13,32] Saskia B. Wortmann,[3,4,8,30,32] and Tobias B. Haack[2,29,32,*]

We report bi-allelic pathogenic *HPDL* variants as a cause of a progressive, pediatric-onset spastic movement disorder with variable clinical presentation. The single-exon gene *HPDL* encodes a protein of unknown function with sequence similarity to 4-hydroxyphenylpyruvate dioxygenase. Exome sequencing studies in 13 families revealed bi-allelic *HPDL* variants in each of the 17 individuals affected with this clinically heterogeneous autosomal-recessive neurological disorder. HPDL levels were significantly reduced in fibroblast cell lines derived from more severely affected individuals, indicating the identified *HPDL* variants resulted in the loss of HPDL protein. Clinical presentation ranged from severe, neonatal-onset neurodevelopmental delay with neuroimaging findings resembling mitochondrial encephalopathy to milder manifestation of adolescent-onset, isolated hereditary spastic paraplegia. All affected individuals developed spasticity predominantly of the lower limbs over the course of the disease. We demonstrated through bioinformatic and cellular studies that HPDL has a mitochondrial localization signal and consequently localizes to mitochondria suggesting a putative role in mitochondrial metabolism. Taken together, these genetic, bioinformatic, and functional studies demonstrate HPDL is a mitochondrial protein, the loss of which causes a clinically variable form of pediatric-onset spastic movement disorder.

The group of pediatric neurological syndromes that include spasticity as the primary feature range from severe spastic movement disorders with onset in infancy to uncomplicated juvenile-onset hereditary spastic paraplegia (HSP). This group of disorders presents challenges to diagnostic paradigms due to large clinical variability and genetic heterogeneity. Delineation of the molecular bases underlying these diseases is necessary for informed decision making and counselling of affected individuals and their families. In addition, there is an increasing number of disorders especially among the inborn errors of metabolism, in which an adjusted clinical management or even new therapeutic approaches directly targeting the pathomechanism convincingly demonstrated

[1]Department of Neuropediatrics, Jena University Hospital, 07747 Jena, Germany; [2]Institute of Medical Genetics and Applied Genomics, University of Tuebingen, 72076 Tübingen, Germany; [3]Institute of Human Genetics, Technical University of Munich (TUM), School of Medicine, 81675 Munich, Germany; [4]Institute of Human Genetics, Helmholtz Zentrum München, 85764 Neuherberg, Germany; [5]Institute of Neurogenomics, Helmholtz Zentrum München, 85764 Neuherberg, Germany; [6]Institute of Human Genetics, Jena University Hospital, 07747 Jena, Germany; [7]Leibniz Institute on Aging - Fritz Lipmann Institute (FLI), 07745 Jena, Germany; [8]University Children's Hospital, Salzburger Landeskliniken (SALK) and Paracelsus Medical University (PMU), 5020 Salzburg, Austria; [9]Department of Neurology, Ben Aknoun Hospital, Benyoucef Benkhedda University, 16028 Algiers, Algeria; [10]Department of Pediatric Neurology, Children's Hospital Datteln, Witten/Herdecke University, 45711 Datteln, Germany; [11]Department of Neurology, Friedrich-Baur-Institute, Ludwig-Maximilians-University, 80336 Munich, Germany; [12]German Center for Neurodegenerative Diseases (DZNE), 81377 Munich, Germany; [13]Department of Pediatric Neurology and Developmental Medicine, University Children's Hospital, 72072 Tübingen, Germany; [14]Clinic for Pediatric Kidney-, Liver- and Metabolic Diseases, Hannover Medical School, 30625 Hannover, Germany; [15]INSERM UMR1163, Developmental Brain Disorders Laboratory, Imagine Institute, Paris-Descartes University, Paris, France; [16]Department of Neurology, Technische Universität München, School of Medicine, 81675 Munich, Germany; [17]Department of Neurology, University of Bonn, 53127 Bonn, Germany; [18]Cancer Research Center and Department of Medical Genetics, School of Medicine, Semnan University of Medical Sciences, Semnan, Iran; [19]Barrow Neurological Institute, Phoenix Children's Hospital & University of Arizona College of Medicine, Phoenix, AZ 85004, USA; [20]Department of Molecular and Human Genetics, Baylor College of Medicine, Houston, TX 77030, USA; [21]Division of Pediatric Neurology, Department of Pediatrics, University of Alberta, Edmonton, AB T6G 2R3, Canada; [22]Iranian Center of Neurological Research, Neuroscience Institute, Tehran University of Medical Sciences, Tehran, Iran; [23]Yale Center for Genome Analysis, Yale University School of Medicine, West Haven, CT 06516, USA; [24]Genetics Research Center, University of Social Welfare and Rehabilitation Sciences, Tehran, Iran; [25]Department of Neuroradiology, University Hospital Tuebingen, 72072 Tübingen, Germany; [26]Faculty of Biological Sciences, Friedrich Schiller University Jena, 07743 Jena, Germany; [27]Munich Cluster for Systems Neurology (SyNergy), 81377 Munich, Germany; [28]German Center for Neurodegenerative Diseases (DZNE), 53127 Bonn, Germany; [29]Centre for Rare Diseases, University of Tuebingen, 72076 Tübingen, Germany; [30]Radboud Center for Mitochondrial Medicine, Department of Pediatrics, Amalia Children's Hospital, Radboudumc, 6525 GA Nijmegen, the Netherlands
[31]These authors contributed equally to this work
[32]These authors contributed equally to this work
*Correspondence: tobias.haack@med.uni-tuebingen.de
https://doi.org/10.1016/j.ajhg.2020.06.015.

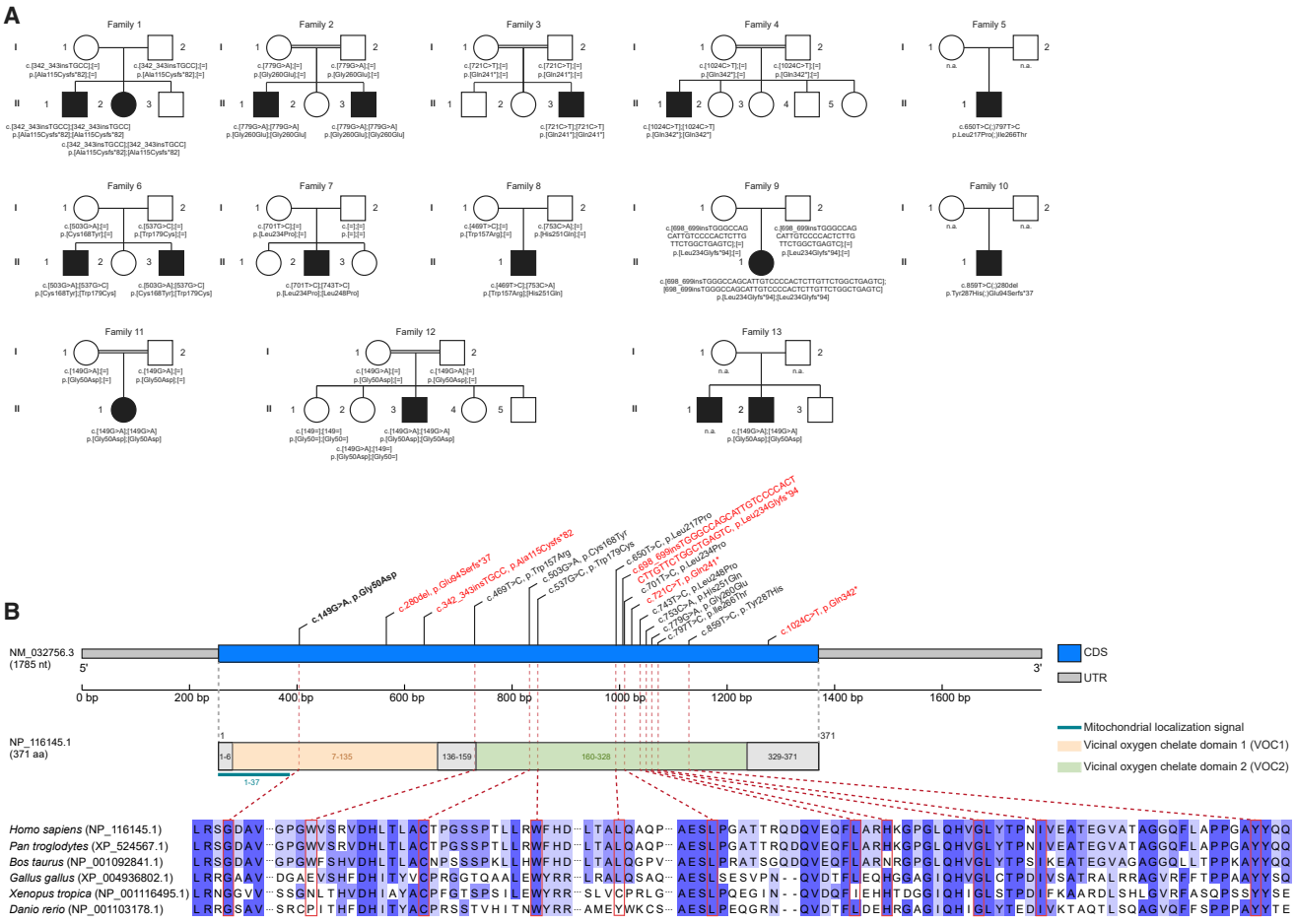

Figure 1. Pedigrees of Investigated Families and Structure of *HPDL*

(A) Pedigrees of 13 families with pathogenic variants in *HPDL*, illustrating the variant carrier status of affected (closed symbols) and healthy (open symbols) family members. Unaffected siblings were not tested unless indicated. n.a., not available for testing.

(B) Gene structure of *HPDL* and structure of the encoded protein with predicted domains of the gene product, mitochondrial localization signal, position of the identified variants, and conservation of affected amino acids across different species. The recurrent variant c.149G>A (p.Gly50Asp) is shown in bold; truncating variants are shown in red. Of note, evidence of the predicted N-terminal VOC domain is rather unclear as it partially overlaps with the mitochondrial localization signal which is expected to be cleaved off. CDS, coding sequence; UTR, untranslated region.

amelioration of clinical signs and symptoms.[1] Although exome and full genome sequencing significantly increased the diagnostic rate in clinical routine, estimates suggest that at least half of the severely affected pediatric cases remain undiagnosed.[2] One explanation among many others is a still incomplete list of disease-associated loci. We report on bi-allelic variants in *HPDL* that cause a spastic movement disorder with broad clinical variability and describe the full range of clinical manifestations resulting from pathogenic *HPDL* variants. *HPDL* is a single-exon gene that encodes a 371 amino acid protein (HPDL [GenBank: NP_116145.1]) of unknown function that is conserved across vertebrates (Figure 1).

Clinical characterization, molecular genetic, bioinformatic, and cell-based functional studies were conducted in 13 families with individuals clinically diagnosed with a pediatric-onset neurological syndrome ranging from a severe spastic movement disorder to uncomplicated HSP. The study was approved by the local ethics committees and informed consent was obtained from all affected individuals or their guardians.

Consanguinity was reported for parents of families F2, F3, F4, F11, and F12 (5 of 13 families, 38%). Pregnancy and postnatal adaption were reportedly normal in all 17 affected individuals. All individuals in this study are alive with current ages ranging from 1 7/12 years to 39 years. Frequently observed clinical findings included chronic progression of neurological signs (n = 16/17, 94%), motor developmental delay (n = 12/17, 71%), intellectual impairment (n = 11/17, 65%), microcephaly (n = 9/16, 56%), and seizures/epilepsy (n = 9/17, 53%). Other relevant clinical findings were visual disturbances/strabismus (n = 9/17, 53%) and loss of developmental milestones (n = 6/17, 35%). Acute central respiratory failure leading to life-threatening events requiring partly mechanically assisted ventilation occurred in half of individuals with infantile presentation (n = 5/10, 50%), respectively one third of all individuals (n = 5/17, 29%). These apnoeas with hypercapnia appeared

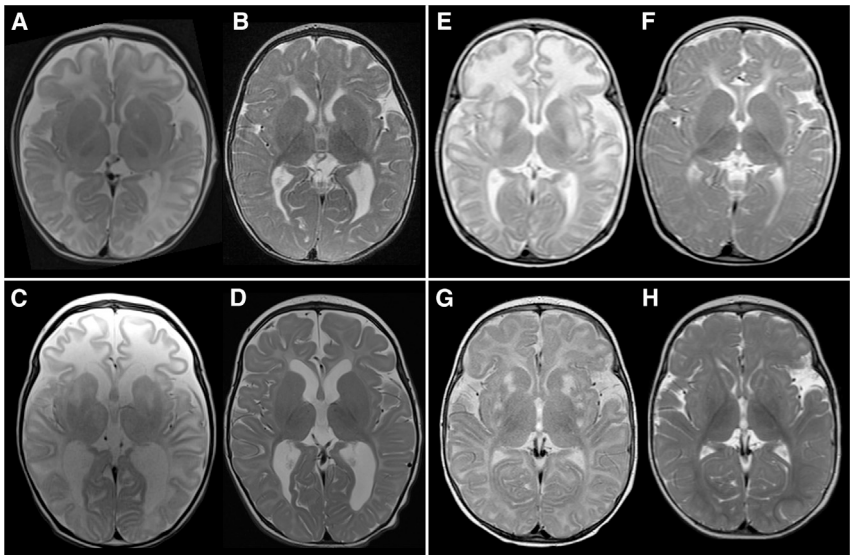

Figure 2. MRI Pattern I
MRIs (T_2-weighted axial scans) from individual F6:II.1 at 2 and 15 months of age (A, B), individual F6:II.3 at 1 1/2 and 7 months of age (C, D), individual F7:II.2 at 2 and 12 months of age (E, F), and individual F8:II.1 at 5 and 12 1/2 months of age (G, H). Early imaging shows multifocal signal increase in the striatum in all individuals, in part associated with swelling (E). With the exception of individual F8:II.1 (G, H), white matter shows abnormal high signal especially in the frontal lobes. On follow-up, myelination in these three individuals is delayed and white matter volume reduced (best seen in B and D).
Summary: after early infantile pathology in the striatum and in part also white matter, follow-up indicates remission of striatal changes, variable progress of myelination, and white matter atrophy if white matter was initially abnormal.

in early infancy (3 resp. 6 weeks of age; F6:II.1 and F6:II.3), childhood (age not specified, F2:II.3), as well as school age (7 and 11 years of age; F4:II.1 and F3:II.3, respectively) with a duration of several days to weeks and without recurrence except in individual F2:II.3 who had two episodes. In individual F3:II.3, acute respiratory failure was reportedly associated with an infection. Demyelinating neuropathy was present in three individuals (n = 3/11, 27%), with reduced sensory nerve conduction velocity (NCV) in all and severely reduced motor NCV in one. Dysmorphic features were documented with high-arched palate and hypertelorism in the two brothers from family F1, a long philtrum and low-set ears in individual F7:II.2, and 2-3 toe syndactyly in individual F11:II.1 (n = 4/17, 24%).

In summary, we observed a spectrum of neurologic impairment ranging from a severe congenital form without any neurological development (n = 2/17, 12%) to infantile-onset presentations (n = 10/17, 59%) with moderate to severe neurodevelopmental issues, partly with a pathology reminiscent of mitochondrial disease (Leigh-like syndrome), to juvenile-onset spastic paraplegia (n = 5/17, 29%).

Elevated lactate in blood (range 2.7–7.9 mmol/l) and/or CSF (range 2.3–8.2 mmol/l) was present in 9 out of 11 (82%) individuals with respective measurements mostly at times of neurologic deterioration but not during check-ups in stable condition. Extensive laboratory testing and metabolic investigations were non-contributory in individuals with corresponding measurements (n = 8/15, 53%). In particular, metabolites of tyrosine degradation (i.e., tyrosine, 4-hydroxyphenylpyruvate) upstream to the HPDL paralog enzyme HPD were normal in blood (n = 7), urine (n = 6), and CSF (n = 6). Moreover, liquid chromatography quadrupole time-of-flight mass spectrometry (LC-QToF-MS) in CSF did not show elevation of tyrosine pathway metabolites (n = 3).[3]

Histology of skeletal muscle displayed fiber size variation in 3 out of 5 (60%) examined individuals. Activities of mitochondrial respiratory chain complexes were variably reduced in skeletal muscle in 2 out of 5 (40%) individuals (Table S1) but not reduced in fibroblasts cell lines from 4 affected individuals (Table S2).

MRI studies of the brain and spinal cord were available for review from 12 and 5 individuals, respectively, in part with longitudinal studies; MR spectroscopy (MRS) was performed on 4 individuals with infantile onset showing elevated lactate peaks in 3 of them (75%). We suggest that three major neuroradiological patterns associated with HPDL deficiency can be delineated (see Figures 2, 3, S1, and S2).

MRI Pattern I (individuals F6:II.1, F6:II.3, F7:II.2, F8:II.1) was characterized by bilateral multifocal striatal signal changes (best seen on T_2-weighted scans), in part with some swelling as well as increased lactate level in MRS in one individual (F6:II.3) evoking a certain acuity. In all but one individual (F8:II.1), myelination was deficient and white matter signal clearly abnormal, indicating white matter pathology. On follow-up, the basal ganglia changes disappeared or were regressive, and an atrophy of the white matter was observed in two individuals (F6:II.1, F6:II.3), although there was some progress in myelination. Two individuals (F7:II.2, F8:II.1) had no atrophy and good myelination progress on follow-up.

Two individuals (F1:II.1 and F1:II.2) with MRI Pattern I Suspected showed severe white matter and corpus callosum volume reduction with parieto-occipital predominance at age 5 (F1:II.1) and 7 (F1:II.2) years (Figure S1). Myelination was deficient; U-fibers particularly were not myelinated (T_2-weighted scans). Cerebellum appeared normal. Taken into account the very early onset of the disease characterized by primary developmental delay and severe neurological signs, and the similarity of MRIs with the later MRI pathology of the two more severely affected individuals with MRI Pattern I (F6:II.1 and F6:II.3), we chose to call this pattern with severe white matter atrophy and deficient myelination MRI Pattern I Suspected,

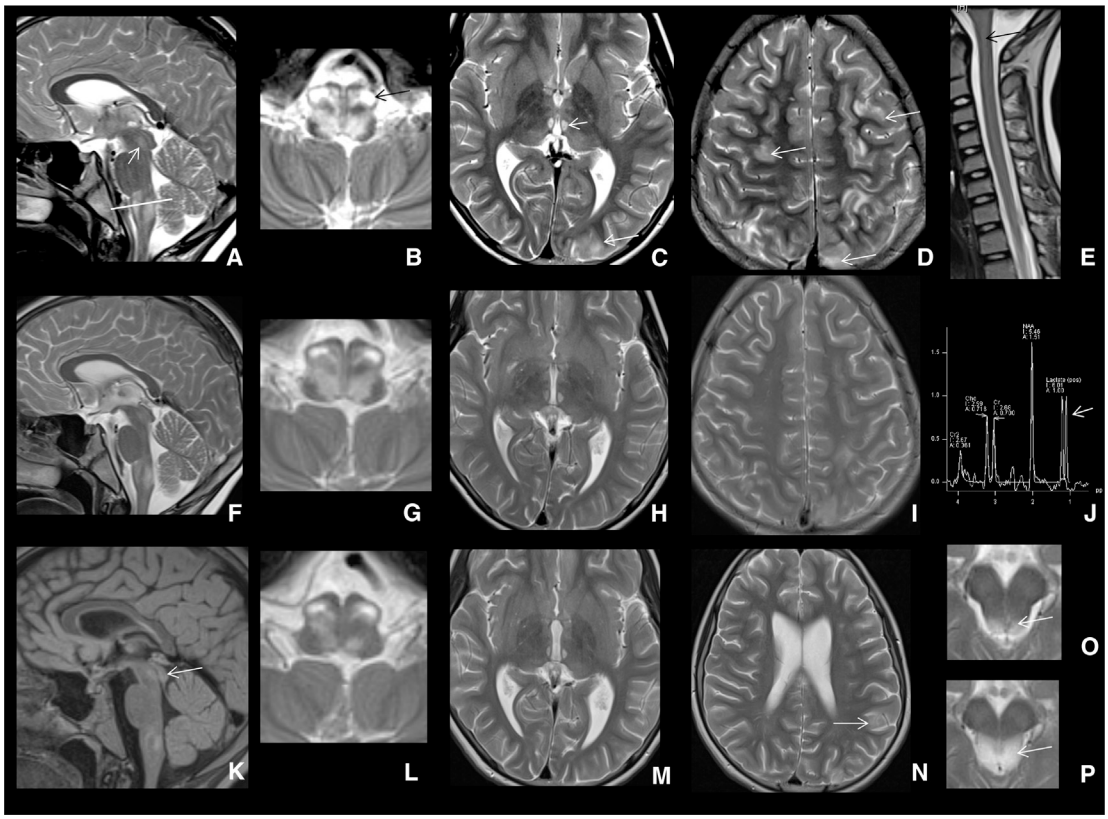

Figure 3. MRI Pattern II

MRIs (T_2-weighted sagittal and axial scans) from individual F3:II.3. At the age of 10 11/12 years (A–E), extensive brain stem involvement is apparent, especially of the olivae (black arrow in B, white line in sagittal image in A indicates position of brainstem in axial image B). The sagittal image also shows diffuse signal changes of the diencephalon and periaquaeductal gray (arrow in A). In the thalamus, distinct changes of the mediodorsal thalamic nuclei are evident (C, short white arrow). Multifocal cortico-subcortical signal changes are indicated by white arrows (C, D). Sagittal images of the spinal cord indicate mild signal increase centrally, most pronounced cervically (black arrow in E). Six days later (F–J), signal changes are overall less prominent and MRS in the frontoparietal white matter shows a lactate peak (arrow, J). At the age of 11 years (K–N), signal changes are further receding, still apparent in colliculi inferiores (arrow in K), brain stem (L), mediodorsal thalamus (M), and some cortical areas (mostly parietal left, arrow in N). Two images of the inferior colliculi at the age of 11 5/12 years (O) and 11 10/12 years (P) show a new pathology bilaterally, getting more prominent and swollen.

Summary: at 11 years of age widespread and acute changes of cortex, thalamus, brain stem, and spinal cord, receding with residual changes in the brain stem; over the course of 11 months, a new pathology appears in the inferior colliculi.

arguing that the early MR signs of MRI Pattern I might have been missed.

MRI Pattern II was observed in two individuals (F3:II.3 and F4:II.1) who showed predominantly brain stem and medioposterior thalamic changes, remitting and relapsing with acute changes of the inferior colliculi. One individual (F4:II.1) also showed cerebellar white matter changes (T_2-weighted scans) as well as increased lactate in the frontoparietal white matter in MRS and the other (F3:II.3) presented with cortico-subcortical changes, which showed in part remission, but relapsed with additional brain stem and inferior colliculi changes. It seems remarkable that no relevant diffusion changes were observed in any affected individual, even when other acute changes were detected.

MRI Pattern III is not related to clear pathology and was found in three individuals (F9:II.3, F11:II.1, and F12:II.3). In one individual (F9:II.3), there was suspicion of long extended central signal changes (T_2-weighted scans) of the spinal cord, which, however, was not confirmed in a follow-up MRI 2 weeks later. Thus, a quickly regressive mild spinal pathology cannot be excluded.

Clinical and genetic findings are summarized in Table 1, pedigrees are shown in Figure 1, and neuroimaging findings are in Figures 2, 3, S1, and S2. Detailed clinical descriptions are provided in the Supplemental Note.

Exome sequencing and analysis were performed at five centers (Tuebingen for families F4, F6, F8, F9, F12, and F13; Munich for families F3, F7, and F11; Baylor for families F5 and F10; Paris for family F1; and Phoenix for family F2) on genomic DNA from individuals F1:II.1, F1:II.2, F2:II.1, F2:II.3, F3:II.3, F4:II.1, F5:II.2, F6:II.1, F6:II.3, F7:II.2, F8:II.1, F9:II.1, F10:II.1, F11:II.1, F12:II.3, and F13:II.2, as well as parental samples from families F3, F4, F6, F8, and F12 as described previously.[4–10] The cohort was assembled using GeneMatcher[11] for families F1, F2, F3, F7, and F11 and by discussion between collaborators for families F4, F5, F6, F8, F9, F10, F12, and F13.

Table 1. Clinical and Genetic Findings in Individuals with Bi-allelic *HPDL* Variants

Individual	F1: II.1	F1:II.2	F2: II.1	F2: II.3	F3: II.3	F4: II.1	F5: II.2	F6: II.1	F6: II.3	F7: II.2	F8: II.1	F9: II.1	F10: II.1	F11: II.1	F12: II.3	F13: II.1	F13: II.2
Gender	M	F	M	M	M	M	M	M	M	M	M	F	M	F	M	M	M
Country of origin	Algeria	Algeria	Iran	Iran	Turkey	Syria	Canada	Ger many	Ger many	Ger many	Ger many	Ger many	USA	Turkey	Syria	Turkey	Turkey
cDNA change[a] variant 1	c.342_343 insTGCC	c.342_343 insTGCC	c.779 G>A	c.779 G>A	c.721 C>T	c.1024 C>T	c.650 T>C	c.503 G>A	c.503 G>A	c.701 T>C	c.469 T>C	c.698_699 insTGGGCC AGCATTG TCCCCACT CTTGTTCT GGCTGAGTC	c.280 del	c.149 G>A	c.149 G>A	N/D	c.149 G>A
Protein change[b] variant 1	p.Ala115 Cysfs*82	p.Ala115 Cysfs*82	p.Gly 260Glu	p.Gly 260Glu	p.Gln 241*	p.Gln 342*	p.Leu 217Pro	p.Cys 168Tyr	p.Cys 168Tyr	p.Leu 234Pro	p.Trp 157Arg	p.Leu234 Glyfs*94	p.Glu94 Serfs*37	p.Gly 50Asp	p.Gly 50Asp	N/D	p.Gly 50Asp
cDNA change[a] variant 2	homo zygous	homo zygous	homo zygous	homo zygous	homo zygous	homo zygous	c.797 T>C	c.537 G>C	c.537 G>C	c.743 T>C	c.753 C>A	homo zygous	c.859 T>C	homo zygous	homo zygous	N/D	homo zygous
Protein change[b] variant 2	homo zygous	homo zygous	homo zygous	homo zygous	homo zygous	homo zygous	p.Ile 266Thr	p.Trp 179Cys	p.Trp 179Cys	p.Leu 248Pro	p.His 251Gln	homo zygous	p.Tyr 287His	homo zygous	homo zygous	N/D	homo zygous
Phenotype	congenital	congenital	infantile	infantile	infantile	infantile	infantile	infantile	infantile	infantile	infantile	infantile	juvenile	juvenile	juvenile	juvenile	juvenile
Age of onset/ current age	congenital/ 8 y	congenital/ 7 y	6 m/ 34 y	2 m/ 21 y	6 m/ 11 y	1 y/ 10 y	1 w/ 22 y	3 w/ 5 y	6 w/ 1 y 7 m	6 w/ 5 y	5 m/ 2 y	5 y/ 8.5 y	15 y/ 17 y	15 y/ 20 y	15 y/ 19 y	14 y/ 39 y	15 y/ 33 y
Delay of motor development	+	+	+	+	+	+	+	+	+	+	+	+	−	−	−	−	−
Intellectual impairment	+ (severe)	+ (severe)	+ (severe)	+ (severe)	+ (moderate)	+ (mild)	+	+ (mild)	N/A	+ (severe)	+ (mild)	+ (mild)	−	−	−	−	−
Chronic progression	+	+	+	+	+	+	+	+	+	−	+	+	+	+	+	+	+
Regression	−	−	+	+	+	+	+	−	−	−	−	+	−	−	−	−	−
Acute respiratory failure (age)	−	−	−	+ (2 x childhood)	+ (11 y)	+ (7 y)	−	+ (3 w)	+ (6 w)	−	−	−	−	−	−	−	−
Microcephaly (SD)	+ (−5.3)	+ (−5.0)	+ (−4.6)	+ (−5.3)	−	−	−	+ (−3.3)	+ (−4.2)	+ (−2.5)	+ (−2.2)	+ (−2)	−	N/D	−	−	−
Seizures	+	+	+	+	+	−	+	+	+	+	−	−	−	−	−	−	−
Spastic paraplegia	+ (tetraparesis)	+ (tetraparesis)	+ (tetraparesis)	+ (tetraparesis)	+	+	+	+	+	+	+	+	+	+	+	+	+

(*Continued on next page*)

Table 1. ***Continued***

Individual	F1: II.1	F1:II.2	F2: II.1	F2: II.3	F3: II.3	F4: II.1	F5: II.2	F6: II.1	F6: II.3	F7: II.2	F8: II.1	F9: II.1	F10: II.1	F11: II.1	F12: II.3	F13: II.1	F13: II.2
Visual disturbance	+	+	−	−	+	+	+	+	+	−	+	−	−	−	−	+	−
MRI pattern	pattern I suspected	pattern I suspected	N/D	pattern I suspected	pattern II	pattern II	#	pattern I	pattern I	pattern I	pattern I	pattern III	#	pattern III	pattern III	N/D	#
lactate increase (MRS)	N/D	N/D	N/D	N/D	+	+	N/D	N/D	+	N/D	−	N/D	N/D	N/D	N/D	N/D	N/D
Peak lactate blood; csf (mmol/l)	2.7; n	n; 6.2	N/D	N/D	5.2; 2.7	n; n	4.3; N/D	4.0; 6.9	7.9; 8.2	N/D; 3.8	4.3; 3.3	n; 2.3	N/D	n; N/D	n; n	N/D	N/D
Nerve conduction studies	n	n	n	n	n	severely reduced motor NCV, slightly reduced sensory NCV	N/D	reduced sensory NCV unilateral	reduced sensory NCV	N/D	N/D	N/D	N/D	n	n	n	N/D
Muscle histology	N/D	N/D	N/D	N/D	n	abnormal variation in muscle fiber diameter	N/D	N/D	n	abnormal variation in muscle fiber diameter	abnormal variation in muscle fiber diameter	N/D	N/D	N/D	N/D	N/D	N/D
Respiratory chain activities (muscle)	N/D	N/D	N/D	N/D	n	globally reduced (CI-CV)	N/D	N/D	CIV-deficiency	n	n	N/D	N/D	N/D	N/D	N/D	N/D
Respiratory chain activities (fibroblasts)	n (CIII/CV increased)	N/D	N/D	N/D	N/D	n (CIII/CV increased)	N/D	N/D	n (CV increased)	N/D	n	N/D	N/D	N/D	N/D	N/D	N/D

M, male; F, female; y, years; m, months; w, weeks; n, normal; N/A, not applicable; N/D, not done/determined; MRS, MR spectroscopy; NCV, nerve conduction velocity; +, present; −, absent; #, MRI not available for review.
[a]GenBank: NM_032756.3
[b]GenBank: NP_116145.1

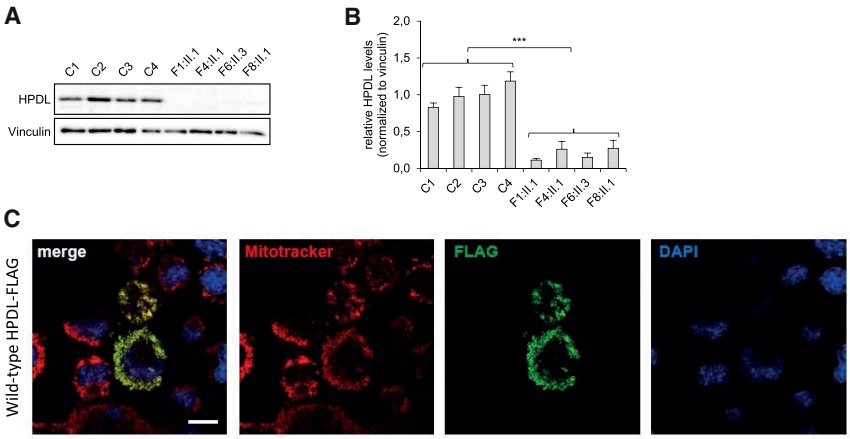

Figure 4. HPDL Protein Levels and Subcellular Localization

(A) Investigation of HPDL protein levels by immunoblot analysis with a polyclonal antibody against full-length HPDL (for detailed methods see Figure S5). HPDL was detected in fibroblasts of control subjects but was significantly reduced in fibroblasts of affected individuals F1:II.1, F4:II.1, F6:II.3, and F8:II.1.

(B) Protein levels were quantified from HPDL immunoblots shown in Figure S5 using ImageJ (NIH). The graph displays the average of three individual experiments ± SEM. Statistics were done using two-tailed t test of the average of the control group compared to the average of affected individuals. ***$p < 0.001$.

(C) Overexpression of *HPDL* cDNA with a C-terminal FLAG tag in N2a cells. Wild-type *HPDL* cDNA was transiently overexpressed and detected by FLAG immunostaining. Mitochondria were stained with Mitotracker and nuclei were stained with DAPI. HPDL co-localizes with the mitochondria. Scale bar = 10 μm.

Clinical genetic diagnostic testing did not reveal pathogenic or likely pathogenic variants in genes that have been associated with the affected individuals' clinical phenotypes and deeper analysis of exome data was subsequently conducted. Due to the presence of consanguinity in several families, rare, bi-allelic non-synonymous variants were prioritized. Variant filtering criteria included minor allele frequency threshold < 0.001, without homozygous occurrence in the Genome Aggregation Database (gnomAD v.2.1.1) as well as in-house exome and genome datasets from individuals with unrelated phenotypes. This search led us to prioritize bi-allelic variants in *HPDL* in all affected individuals ($n = 17$) in this cohort of 13 unrelated families (Figure 1). No homozygous loss-of-function variants in *HPDL* were listed in gnomAD (v.2.1.1) or individuals with unrelated phenotypes in in-house databases. Segregation analyses on available family members showed full co-segregation of the identified bi-allelic *HPDL* variants with the clinical status in all families (Figure 1A).

The 17 affected individuals were either homozygous or compound heterozygous for ultra-rare variants in *HPDL* (Table 1). Across these 17 affected individuals, 16 *HPDL* unique variants were identified, only one of which was observed in gnomAD: the missense variant *HPDL* (GenBank: NM_032756.3): c.149G>A (p.Gly50Asp) was detected twice in a heterozygous state in the non-Finnish European population and has an allele frequency of 1e−5 in the total gnomAD population. Five of the identified variants are nonsense variants. Given that *HPDL* is a single-exon gene, the mutant messenger RNAs are likely to escape nonsense-mediated decay resulting in a prematurely truncated polypeptide and loss of HPDL function. A total of 11 *HPDL* missense variants were observed in this cohort. All missense variants affect evolutionarily conserved amino acids, with most of them being highly conserved (phyloP), and are predicted pathogenic *in silico* (10/11 variants predicted deleterious with SIFT score ≤ 0.01, 9/11 variants predicted probably damaging with PolyPhen score > 0.9, CADD score > 18 for 11/11 variants and > 25 for 8/11 variants) (Figure 1, Table S3).

One missense variant, c.149G>A (p.Gly50Asp), was observed in a homozygous state in four affected individuals from the three families F11, F12, and F13. Concordant with the reported consanguineous relationships in families F11 and F12 and a presumed distant relatedness in family F13, we detected extended runs of homozygosity (ROH) including ~8.4 Mb, ~4.9 Mb, and ~3.3 Mb of ROH encompassing *HPDL*. These families originate from neighboring geographic regions in Turkey and Syria. The analysis of the genomic region surrounding *HPDL* showed that the affected individuals from these families share the same homozygous common variants over a 1.9 Mb region that traverses *HPDL* and includes 58 segregating variants with the respective positions being covered in all three exome datasets (Table S4). These data are in line with a distant shared ancestry among these families.

Of note, the missense variant c.149G>A (p.Gly50Asp) is consistently associated with isolated spastic paraplegia evolving in the second decade of life and currently no additional pathologies. Apart from one additional individual with a juvenile presentation (F10:II.1), the remaining affected individuals reported in this study had a more severe, infantile-onset disease presentation. We speculate that the milder clinical presentation observed in a subset of affected individuals with predominant spastic paraplegia evolving in the second decade of life might result from putative residual activities in some HPDL mutants. However, at the time of the study no biomaterials from any of these individuals were available to confirm the postulated presence of residual amounts of HPDL. Furthermore, to our knowledge, the molecular function of HPDL is currently unknown and the lack of a direct test for HPDL function or biomarker currently prevents a detailed evaluation of correlations between genotypes, residual protein function, and phenotypic spectrum.

We tested the hypothesis that *HPDL* variants detected in severely affected individuals caused loss of function.

Fibroblast cell lines were available from four affected individuals, F1:II.1, F4:II.1, F6:II.3, and F8:II.1, to perform additional studies to test the functional relevance of identified variants. Western blot analyses showed a significant reduction in HPDL protein levels in fibroblasts from affected individuals compared to control fibroblasts (Figure 4). This result demonstrates that the *HPDL* variants detected in these individuals resulted in the severe reduction of HPDL protein. Given that the mutant mRNA of the single-exon gene *HPDL* should escape nonsense-mediated decay, the nonsense variants detected in individuals F1:II.1 and F4:II.1 presumably lead to a loss of HPDL via impaired protein stability. The other two individuals tested here, F6:II.3 and F8:II.1, were compound heterozygous for missense variants and our results indicate that, similar to nonsense variants, the identified missense changes result in loss of function of HPDL (Figure S5). We hypothesize that these missense changes result in loss of HPDL through impaired production or stability of the HPDL protein.

HPDL is present in various tissues with particularly high levels in the central and peripheral nervous system (GTEx Analysis Release V.8, dbGaP Accession phs000424.v8.p2 on 03/10/2020). The function of HPDL is currently unknown. Bioinformatic analysis shows that HPDL belongs to the vicinal oxygen chelate (VOC) superfamily. VOC members are metalloenzymes with diverging sequence and biological functions, commonly sharing a βαββββ structural motif (VOC fold), that form an incompletely closed barrel of β sheet around a metal ion.[12] The Human Protein Atlas reports HPDL as having mitochondrial localization, based on antibody-based profiling by immunofluorescence confocal microscopy.[13] However, HPDL is not present in the MitoCarta2.0, which is a database of 1,158 human proteins with mass-spectometry-based evidence of localization to the mitochondria.[14] To resolve these conflicting reports, we carried out bioinformatic and functional studies. First, we conducted bioinformatic analysis, using MitoProt II, to determine if the HPDL protein sequence contains a mitochondrial localization signal.[15] MitoProt II predicts that the first 37 amino acids of HPDL comprise a mitochondrial localization signal (Figure 1), with 98% probability. Next, we overexpressed wild-type *HPDL* cDNA in a murine Neuro 2A cell line and performed immunohistological studies visualizing HPDL with a C-terminal FLAG tag. The results of these experiments demonstrate that HPDL co-localizes with the mitochondria as shown in Figure 4.

Having established a mitochondrial localization of HPDL, we assessed whether HPDL might play a role in oxidative phosphorylation (OXPHOS) and whether loss of HPDL leads to disruption of the mitochondrial network. Investigation of mitochondrial morphology in fibroblasts from affected individuals visualized by Mitotracker Red CMXRos staining and data analysis with the Mitochondrial Network Analysis (MiNA[16]) tool showed no significant differences between control and fibroblast cell lines from affected individuals (n = 2/2, Figures S3 and S4). As stated previously, analyses of the OXPHOS component enzyme activities showed mostly normal activities in fibroblasts from affected individuals (n = 4, Table S2). In line with this observation, immunofluorescence studies in fibroblasts from affected individuals of OXPHOS subunits including NDUFS4, SDHA, UQCRC2, MT-CO1, and ATP5F1A (data not shown) as well as immunoblot analysis of NDUFB8, SDHB, UQCRC2, COX IV, and ATP5A in fibroblasts from affected individuals (Figure S6) failed to show any consistent abnormalities. Analysis of OXPHOS complexes in available skeletal muscle specimen revealed variably decreased activities of complexes I and/or IV in some individuals (n = 2/5, Table S2). Muscle biopsies were reported displaying abnormal variation in muscle fiber diameter in the majority of investigated cases (n = 3/5, 60%, data not shown). Immunohistochemical staining of muscle tissue from two affected individuals (F4:II.1 and F6:II.3) indicated overall lower levels of mitochondrial/OXPHOS proteins (VDAC1, SDHA, and MT-CO1) in comparison to control subjects (Figure S7), whereby it was remarkable that large muscle bundles of F4:II.1 had a depletion of mitochondria. Consistent with this observation, western blot analyses of muscle tissue showed a general lack of OXPHOS enzymes in F4:II.1 but not in F8:II.1 (Figure S8). Together, these data fail to establish a consistent signature of OXPHOS impairment or mitochondrial dysmorphology in the investigated fibroblasts or muscle from affected individuals.

In summary, the identification of 16 different bi-allelic functionally relevant *HPDL* variants in 17 affected individuals from 13 unrelated families establishes *HPDL* as a gene confidently implicated in this neurological disorder. In all individuals a spastic movement disorder predominantly of the lower limbs was observed as a common clinical sign. However, disease onset and progress as well as the spectrum of accompanying phenotypes were highly variable. The most severely affected individuals had a congenital disease onset with primary microcephaly and severe developmental delay but without clearly progressive neurological signs and an overall stable disease course. Affected individuals with infantile-onset disease manifested first signs and symptoms after weeks, months or even years of apparently normal development. Clinical and neuroimaging findings in these individuals initially resembled mitochondrial encephalopathies. However, compared with other forms of mitochondrial disease, such as complex I-associated Leigh syndrome, the further clinical course seems to be more stable resulting in a spastic movement disorder with additional features such as intellectual disability, epilepsy, swallowing problems, and peripheral neuropathy. A third group includes individuals who are homozygotes for the missense change c.149G>A (p.Gly50Asp) that develop hereditary spastic paraplegia between the ages of 14 and 15 years without obvious abnormalities in brain and spinal MRI or additional clinical features. Our study highlights the broad heterogeneity of clinical features associated with HPDL deficiency rendering this disorder an important differential diagnosis for a substantial fraction of clinical conditions managed by pediatric as well as adult neurologists. However, further

studies and long-term follow-up of affected HPDL individuals are needed to fully define the phenotypic spectrum and natural disease course associated with HPDL deficiency. Of note, the disease course of several individuals is compatible with a relatively acute exacerbation of the disease followed by a static encephalopathy and development of a residual clinical status hallmarked by a spastic movement disorder. Comparable disease courses are known from other metabolic disorders including ECHS1 deficiency, a defect presumably exerting its effect due to accumulation of toxic metabolites and secondary impairment of the OXPHOS machinery and mitochondrial metabolism.[17] Along this line, acute episodes might be triggered by external factors such as infection or nutritional status and vice versa might be amenable to early symptomatic or even dietary intervention. Key to the development of any therapeutic approach is a better understanding of the physiological function of HPDL and, if deficient, the downstream molecular cascades causing pathology. Our clinical observations and functional studies suggest an involvement of mitochondrial metabolism in the pathogenesis of the disease. These include biochemical features like elevated lactate and alanine in body fluids, neuroimaging findings with bilateral signal alterations of the basal ganglia and brain stem, lactate elevation in MR spectroscopy, as well as experimental evidence of a mitochondrial localization of HPDL. However, we did not observe a consistent signature of mitochondrial dysfunction in HPDL mutant fibroblasts and skeletal muscle. As stated above, a potential explanation could be that mitochondrial function is only secondarily impaired during acute episodes of the disease and cannot be directly confirmed at later time points *in vivo* or by using *in vitro* model systems such as fibroblast cell lines. Furthermore, the clinically predominantly affected organ is the brain and probably more advanced approaches such as neuronal cell lines or organoids are needed to model and eventually understand HPDL deficiency in more detail.

Data and Code Availability

This study did not generate new code. Sequence datasets have been generated and contributed by different study sites and have not been deposited in a public repository due to varying local consent regulations. Selected datasets might be available from the corresponding author on request.

Supplemental Data

Supplemental Data can be found online at https://doi.org/10.1016/j.ajhg.2020.06.015.

Acknowledgments

We thank all families for their participation. We thank Karlien Coene, PhD, Department of Laboratory Medicine, Translational Metabolic Laboratory, Radboud University Medical Center, Nijmegen, the Netherlands for next-generation metabolic screening of CSF. T.B.H. was supported by the German Bundesministerium für Bildung und Forschung (BMBF) through the Juniorverbund in der Systemmedizin "mitOmics" (FKZ 01ZX1405C), the intramural fortüne program (#2435-0-0), and by the Deutsche Forschungsgemeinschaft (DFG, German Research Foundation) – Projektnummer (418081722). S.B.W. was supported by the Jubiläumsfonds of the OeNB Nr. 18023. J.A.M. was supported by the E-Rare project GENOMIT FWF-I2741B26. C.A.H. was supported by the BMBF (TreatHSP, FKZ 01GM1905D). F.R., T.M., and T. Klopstock were supported by a German Federal Ministry of Education and Research grant to the German Network for Mitochondrial Disorders (mitoNET, 01GM1113A, and 01GM1906A). P.E.B. was supported by NIH NINDS RO1 NS08372. Several authors of this publication are members of the European Reference Network for Rare Neurological Diseases - Project ID No 739510.

Declaration of Interests

The authors declare no competing interests.

Received: May 18, 2020
Accepted: June 22, 2020
Published: July 23, 2020

Web Resources

Ensembl Variant Effect Predictor, https://grch37.ensembl.org/Homo_sapiens/Tools/VEP
CADD, https://cadd.gs.washington.edu/
GenBank, https://www.ncbi.nlm.nih.gov/genbank/
gnomAD Browser, https://gnomad.broadinstitute.org/
GTEx Portal, https://gtexportal.org
MitoProt II, https://ihg.gsf.de/ihg/mitoprot.html
OMIM, https://www.omim.org/
The Human Protein Atlas, http://www.proteinatlas.org/
UCSC (February 2009), https://genome.ucsc.edu

References

1. Koch, J., Mayr, J.A., Alhaddad, B., Rauscher, C., Bierau, J., Kovacs-Nagy, R., Coene, K.L., Bader, I., Holzhacker, M., Prokisch, H., et al. (2017). CAD mutations and uridine-responsive epileptic encephalopathy. Brain *140*, 279–286.
2. Lionel, A.C., Costain, G., Monfared, N., Walker, S., Reuter, M.S., Hosseini, S.M., Thiruvahindrapuram, B., Merico, D., Jobling, R., Nalpathamkalam, T., et al. (2018). Improved diagnostic yield compared with targeted gene sequencing panels suggests a role for whole-genome sequencing as a first-tier genetic test. Genet. Med. *20*, 435–443.
3. Coene, K.L.M., Kluijtmans, L.A.J., van der Heeft, E., Engelke, U.F.H., de Boer, S., Hoegen, B., Kwast, H.J.T., van de Vorst, M., Huigen, M.C.D.G., Keularts, I.M.L.W., et al. (2018). Next-generation metabolic screening: targeted and untargeted metabolomics for the diagnosis of inborn errors of metabolism in individual patients. J. Inherit. Metab. Dis. *41*, 337–353.
4. Haack, T.B., Hogarth, P., Kruer, M.C., Gregory, A., Wieland, T., Schwarzmayr, T., Graf, E., Sanford, L., Meyer, E., Kara, E., et al. (2012). Exome sequencing reveals de novo WDR45 mutations causing a phenotypically distinct, X-linked dominant form of NBIA. Am. J. Hum. Genet. *91*, 1144–1149.

5. Ploski, R., Pollak, A., Müller, S., Franaszczyk, M., Michalak, E., Kosinska, J., Stawinski, P., Spiewak, M., Seggewiss, H., and Bilinska, Z.T. (2014). Does p.Q247X in TRIM63 cause human hypertrophic cardiomyopathy? Circ. Res. *114*, e2–e5.
6. Yang, Y., Muzny, D.M., Xia, F., Niu, Z., Person, R., Ding, Y., Ward, P., Braxton, A., Wang, M., Buhay, C., et al. (2014). Molecular findings among patients referred for clinical whole-exome sequencing. JAMA *312*, 1870–1879.
7. Fritzen, D., Kuechler, A., Grimmel, M., Becker, J., Peters, S., Sturm, M., Hundertmark, H., Schmidt, A., Kreiß, M., Strom, T.M., et al. (2018). De novo FBXO11 mutations are associated with intellectual disability and behavioural anomalies. Hum. Genet. *137*, 401–411.
8. Kremer, L.S., Bader, D.M., Mertes, C., Kopajtich, R., Pichler, G., Iuso, A., Haack, T.B., Graf, E., Schwarzmayr, T., Terrile, C., et al. (2017). Genetic diagnosis of Mendelian disorders via RNA sequencing. Nat. Commun. *8*, 15824.
9. Wagner, M., Berutti, R., Lorenz-Depiereux, B., Graf, E., Eckstein, G., Mayr, J.A., Meitinger, T., Ahting, U., Prokisch, H., Strom, T.M., and Wortmann, S.B. (2019). Mitochondrial DNA mutation analysis from exome sequencing-A more holistic approach in diagnostics of suspected mitochondrial disease. J. Inherit. Metab. Dis. *42*, 909–917.
10. Alby, C., Boutaud, L., Bessières, B., Serre, V., Rio, M., Cormier-Daire, V., de Oliveira, J., Ichkou, A., Mouthon, L., Gordon, C.T., et al. (2018). Novel de novo ZBTB20 mutations in three cases with Primrose syndrome and constant corpus callosum anomalies. Am. J. Med. Genet. A. *176*, 1091–1098.
11. Sobreira, N., Schiettecatte, F., Valle, D., and Hamosh, A. (2015). GeneMatcher: a matching tool for connecting investigators with an interest in the same gene. Hum. Mutat. *36*, 928–930.
12. He, P., and Moran, G.R. (2011). Structural and mechanistic comparisons of the metal-binding members of the vicinal oxygen chelate (VOC) superfamily. J. Inorg. Biochem. *105*, 1259–1272.
13. Thul, P.J., Åkesson, L., Wiking, M., Mahdessian, D., Geladaki, A., Ait Blal, H., Alm, T., Asplund, A., Björk, L., Breckels, L.M., et al. (2017). A subcellular map of the human proteome. Science *356*, 356.
14. Calvo, S.E., Clauser, K.R., and Mootha, V.K. (2016). MitoCarta2.0: an updated inventory of mammalian mitochondrial proteins. Nucleic Acids Res. *44* (D1), D1251–D1257.
15. Claros, M.G., and Vincens, P. (1996). Computational method to predict mitochondrially imported proteins and their targeting sequences. Eur. J. Biochem. *241*, 779–786.
16. Valente, A.J., Maddalena, L.A., Robb, E.L., Moradi, F., and Stuart, J.A. (2017). A simple ImageJ macro tool for analyzing mitochondrial network morphology in mammalian cell culture. Acta Histochem. *119*, 315–326.
17. Haack, T.B., Jackson, C.B., Murayama, K., Kremer, L.S., Schaller, A., Kotzaeridou, U., de Vries, M.C., Schottmann, G., Santra, S., Büchner, B., et al. (2015). Deficiency of ECHS1 causes mitochondrial encephalopathy with cardiac involvement. Ann. Clin. Transl. Neurol. *2*, 492–509.